

I. PHYSICAL ELECTRONICS

Prof. W. B. Nottingham
S. Aisenberg
D. H. Dickey

J. M. Houston
W. J. Lange

R. D. Larrabee
H. Shelton
L. E. Sprague

RESEARCH OBJECTIVES

The study of those properties of electrons that are not specifically associated with individual atoms forms the basis of the science of physical electronics. Examples of investigations carried out under this program include:

1. thermionic emission from pure materials – tungsten and complex composite surfaces, for example – including, specifically, the oxide cathode;
2. photoelectric emission from insulators and semiconductors as well as from pure surfaces;
3. strong-field emission from single crystals and a detailed analysis of the field emission dependence on crystallographic direction and temperature;
4. properties of low pressure gas discharges.

Other subjects suitable for investigation include surface properties of semiconductors, photoconductive and photovoltaic effects, and secondary electron emission from all kinds of solids, including conductors, semiconductors, and insulators.

The recently finished project on the thermionic properties of tungsten yielded new data on the differences in the true thermionic work-function for the different crystallographic directions in a single crystal of tungsten. This study also revealed by direct measurement the fact that the electrons emitted from the filament do not have the distribution in energy which might be expected from elementary theoretical considerations. The experiments indicate that there is a very considerable deficiency of slow electrons in the energy group between zero and one electron volt with a greater and greater deficiency as the energy decreases. This result confirms previous studies made by an entirely different method. We would have an explanation for this observed deficiency if it were clearly established that very slow electrons reflect from single crystal surfaces. It is therefore of great importance that an unambiguous experiment be undertaken to evaluate this hypothesis.

The quality of work in this field depends upon the development and improvement of experimental techniques as they relate to the production of suitable specimens for investigation and the maintenance of these specimens in the right environment for study. Specifically, vacuum techniques are of the utmost importance, and a continuing program to determine improved means of acquiring ultrahigh vacuum and its measurement is currently under way. One of the most promising projects for the immediate future is the development and evaluation of the MassITron described in this report.

W. B. Nottingham

A. ELECTRON EMISSION PROBLEMS

1. Reflection of Slow Electrons at a Metal Surface

The purpose of this research is to resolve a possible conflict in results concerning reflection at the metal boundary. Calculations (1) based on mathematical models yield a reflection coefficient that increases to a maximum of less than 10 per cent at zero electron energy, while several thermionic emission experiments (2, 3) performed in this laboratory may be interpreted as indicating that the reflection is more important and may rise as high as 100 per cent at zero energy. This conclusion depends on the established fact that there is a deficiency in slow electrons. No experiment in

(I. PHYSICAL ELECTRONICS)

secondary emission has covered the range of primary energies in which the reflection effect is expected. The present experiment is designed to give a direct determination of electron reflection as a function of electron energy.

A magnetic velocity analyzer will provide a primary beam of monoenergetic electrons at energies of less than one electron volt to several electron volts. This beam will strike a clean, smooth, metal surface at normal incidence; any reflected electrons can then be studied with a second analyzer. As the primary energy is varied, the ratio of reflected current to incident current will give the reflection coefficient.

The metal surface must be homogeneous and reproducible for the results to have meaning. For this reason, a single crystal of tantalum which has been smoothed and can be heated in the final assemblage to insure cleanliness is being prepared. The experiment must be performed at high vacuum so that the surface will remain uncontaminated while the measurements are made.

W. J. Lange

References

1. Reviewed by C. Herring and M. H. Nichols, *Revs. Modern Phys.* 21, 185 (1949).
2. W. B. Nottingham, *Phys. Rev.* 49, 78 (1936).
3. A. R. Hutson, Ph.D. Thesis, Department of Physics, M.I. T. (1953).

B. EXPERIMENTAL STUDIES

1. High-Vacuum MassITron

This new ionization gauge serves the purpose for which the Omegatron was designed: the quantitative determination of the partial pressure and composition of gases at low pressure. It is hoped that the MassITron will extend the range of ion identification to partial pressures of 10^{-10} mm Hg.

The small, glass-enclosed, mass spectrometer illustrated in Fig. I-1 is designed to

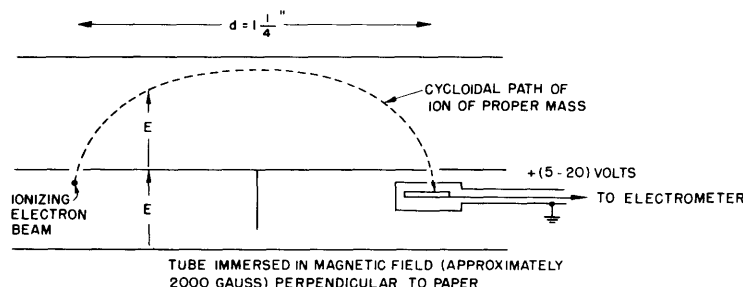


Fig. I-1
The MassITron.

fit the gap of a permanent magnet. It is made out of nonmagnetic parts so mounted that they can be thoroughly cleaned by high-frequency induction heating. Shielding and insulation are so designed that currents as low as 10^{-15} amp can be measured. The electron beam is parallel to the magnetic field, with the source and collector hidden from the main chamber. All ions formed with small random speeds in any direction will follow cycloidal paths. Ions of a particular mass take the path shown in the figure. The defining equation is $E_m = de B^2/2\pi$, where E is the electric field in volts per meter; m is the ion mass in kilograms; d is the distance in meters; and B is the magnetic field in webers per square meter.

H. Shelton

2. The Spectral Emissivity of Tungsten

An experiment designed to measure the spectral emissivity of tungsten at incandescent temperatures has been initiated. A direct-comparison method will be utilized in which the radiant intensity from the tungsten source is compared with the radiant intensity from an approximating black body, and the spectral emissivity is computed by the basic relation

$$E_{\lambda T} = \frac{S}{B} \quad (1)$$

where $E_{\lambda T}$ is the spectral emissivity at temperature T and wavelength λ , S is the radiant intensity of the tungsten source, and B is the radiant intensity of the approximating black body.

The approximating black-body source under construction is a hollow tungsten cylinder that is 1/8 inch in diameter, is 4 inches long, and has a wall thickness of 1 mil. The cylinder has a 12-mil (diameter) hole in its lateral surface that serves as the source of black-body radiation. When the cylinder is heated to incandescence by the passage of direct current, the small wall thickness assures that negligible temperature differences will develop between the inside and outside wall surfaces. Consequently, a selected spot on the outside surface of the cylinder will serve as the tungsten source in question (see Fig. I-2).

The light whose radiant intensity is to be measured is separated from the remaining undesired light by an optical system consisting of a lens and a limiting aperture which forms the "entrance slit" of a monochromator. The light passing through the monochromator falls upon a type 931 photomultiplier and its intensity is measured to three-figure accuracy.

A correction, however, must be made for scattered light. A through hole backed by an exponentially shaped horn (Fig. I-2) may be aligned with the optic axis of the lens system for the purpose of measuring this scattered component of radiation (which

(I. PHYSICAL ELECTRONICS)

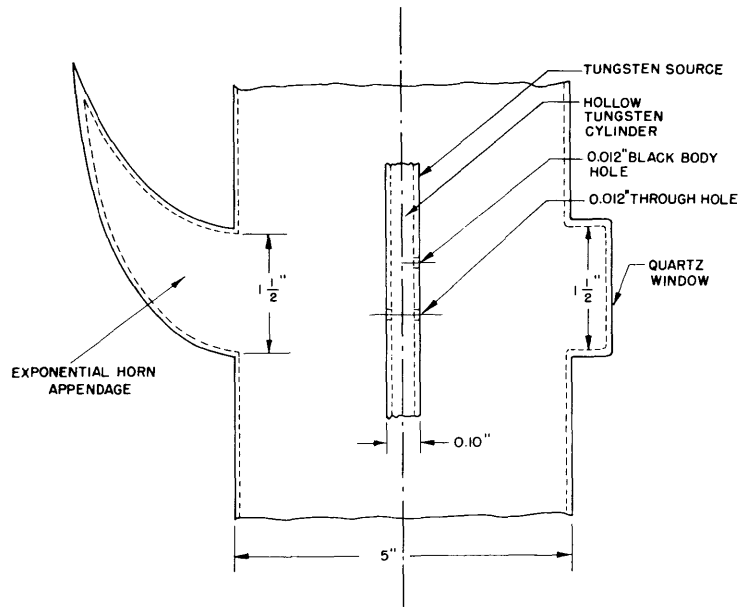


Fig. I-2

Side view of central portion of the emissivity tube.
 (For clarity, the diameter of the tungsten cylinder
 has been drawn too large by a factor of 5.)

amounts to about 5-15 per cent of the measured light). If this through-hole reading of the photometer is represented by α , the emissivity is given by

$$E_{\lambda T} = \frac{S}{B} = \frac{S' - \alpha}{B' - \alpha} \quad (2)$$

where S' and B' are the uncorrected photometer readings for the tungsten source and the black-body hole.

R. D. Larrabee

3. Cleanup of Helium in Ionization Gauges

The phenomenon of cleanup of helium in the Bayard-Alpert ionization gauge has been studied for approximately a year. From this work has been evolved a theory that will predict the form of the experimental curves of both cleanup and re-entrance. Two essential assumptions are that the cleanup is due to single ions of helium and that a fraction of the ions cleaned up are returned to the ionizing space. This theory predicts cleanup curves of the form of two exponentials; that is, if the number of helium atoms in the ionizing region, N_s , is plotted against time, t , the following cleanup curve is predicted:

$$(N_s - N_\infty) = c_1 e^{+r_1 t} + c_2 e^{+r_2 t} \quad (1)$$

where r_1 and r_2 are functions of the electron collector current (i), the temperature (T), and other constants of the gauge. N_∞ is the equilibrium value of N_s for large values of time and a constant for a particular cleanup curve. This theory also predicts curves of the re-entrance of helium atoms to the ionizing space, while the gauge is nonoperative, of the form:

$$N_s = c_4(1 - e^{-\beta t}) + N_{s_0} + P(T)t \quad (2)$$

where it is seen that $N_s = N_{s_0}$ at $t = 0$.

Observed curves are found to follow the above equation. Also, all cleanup curves are found to be nearly the sum of two exponentials. Electron collector voltages and currents for which these results have been found are 40, 60, and 90 volts, and currents of 100 to 500 μ a.

It has been observed that the equilibrium value of the concentration (N_∞) is inversely proportional to the electron current. This result is consistent with theory.

There are still many unknown factors involved in the operation of the Bayard-Alpert ionization gauge. One puzzling characteristic now being investigated is the change of the roots r_1 and r_2 of the cleanup curve with the length of time since the bake-out of the tube. It has been observed in one tube that the roots r_1 and r_2 decreased by a factor of about two over a period of six months. Such a variation has not yet been accounted for.

D. H. Dickey

4. Ionization Gauge Control Circuit

A detailed description will be given of some of the features of the ionization gauge control circuit. Knowledge of the electron current i_- and the ion current i_+ is required

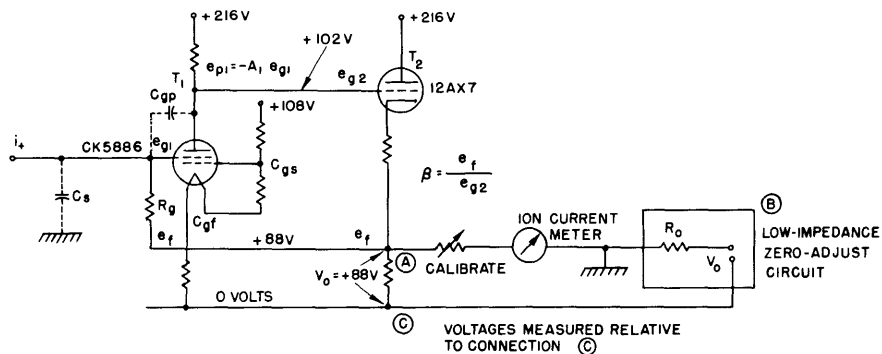


Fig. I-3

Vacuum tube electrometer.

(I. PHYSICAL ELECTRONICS)

for the measurement of low pressures by means of an ionization gauge and the relationship $p = (i_+/i_-)/K$ (where p is the pressure in mm Hg, and K is the gauge constant that depends upon the gauge geometry, electrode potentials, and the gas). Since the electron current will be between $10 \mu\text{a}$ and 10ma , it can be measured by means of a $100\text{-}\mu\text{a}$ panel meter associated with appropriate shunting resistors. Measurement of the ion current i_+ is more difficult, since the ion current is low and will be between 10^{-5} amp and 10^{-12} amp. This small current is measured by means of a vacuum tube electrometer circuit, illustrated in Fig. I-3.

The principle of operation of the electrometer circuit is as follows: The ion current i_+ to be measured is passed through the grid resistor R_g , selected by a range switch from a set of resistors varying from 10^6 ohms to 10^{11} ohms. This current develops a voltage $R_g i_+$ (one volt full-scale). A feedback voltage e_f , representing a change from the zero signal voltage V_0 at point A, results in a signal $e_{g1} = e_f + R_g i_+$ to the grid of the electrometer tube. If the gain of the electrometer tube circuit is $A_1 = -(e_{p1}/e_{g1})$ ($A_1 \approx 120$ in the present circuit), the signal applied to the grid of the cathode follower is $e_{g2} = -A_1(e_f + R_g i_+)$. A fraction β ($\beta \approx 1/4$ in the present case) of e_{g2} is fed back into the grid of the electrometer tube. It can be seen that the feedback is negative, and this relationship holds:

$$e_f = \beta e_{g2} = -\beta A_1 (e_f + R_g i_+)$$

or

$$i_+ R_g = -e_f \left(1 + \frac{1}{\beta A_1} \right)$$

Thus it can be seen that measurement of e_f plus a knowledge of R_g will yield the value of i_+ without the need for extreme stability of βA_1 , since βA_1 can change by approximately

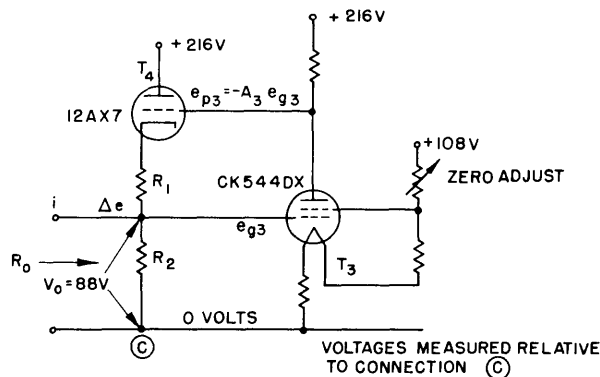


Fig. I-4

Low-impedance, zero-adjust network.

25 per cent and result in a 1 per cent error in the value of i_+ .

It can be shown that the input capacity with negative feedback is given by

$$C_i = \frac{C_s(1 + \gamma\beta A_1) + C_{gp}(1 + A_1) + C_{gf} + C_{gs}}{1 + \beta A_1}$$

where $\gamma = R_o/R_T$, and R_o , approximately 300 ohms, is the input resistance of the network that serves to "buck out" the zero signal voltage V_o . The resistance R_T , of approximately 10,000 ohms, is the total resistance in the circuit branch from A to B to C (which contains the ion current meter and R_o). When compared with the input capacity without feedback

$$C_i = C_s + C_{gp}(1 + A_1) + C_{gf} + C_{gs}$$

it is seen that the feedback reduces the input cable capacity C_s , and the Miller-effect capacity. The time constant on the most sensitive range ($R_g = 10^{11}$ ohms) is approximately 1 sec or about a factor of 20 smaller than it would be without feedback.

The next important feature of the circuit is the low-impedance, zero-adjust network that takes the place of a "bucking battery" and which is therefore partially responsible for the gain and zero stability of the circuit. This low-impedance network is illustrated in Fig. I-4, and the input impedance R_o is given by

$$\frac{1}{R_o} = \frac{1}{R_2} + \frac{\mu_4(1 + A_3) + 1}{V_{p4} + (\mu_4 + 1)R_1}$$

For the circuit that is actually used

$$R_o \approx \frac{R_1 + \frac{1}{g_{m4}}}{A_3}$$

which yields a numerical value of about 300 ohms for R_o . This low input impedance is achieved, of course, by means of negative feedback within the network.

More detailed information is available from Research Laboratory of Electronics drawings A-1503-1 and B-1504-1. A set of operating, construction, and alignment instructions is being prepared.

S. Aisenberg